

## The Effects of Nano MgO on Physical and Mechanical Properties of Al<sub>2</sub>O<sub>3</sub>-SiC Composites

A. Nemati<sup>\*1</sup>, F. Surani<sup>2</sup>, H. Abdizadeh<sup>3</sup> and H.R. Baharvandi<sup>4</sup>

<sup>1</sup>Department of Materials Science and Engineering, Sharif University of Technology, Azadi St., Tehran, Iran

<sup>2</sup>Department of Materials Engineering, Science and Research Branch, IAU, Tehran, Iran

<sup>3</sup>School of Metallurgy and Materials Engineering, University of Tehran, Tehran, Iran

<sup>4</sup>Malek Ashtar University of Technology, Tehran, Iran

received August 28, 2011; received in revised form January 5, 2012; accepted January 19, 2012

### Abstract

In this research, the effects of nano-sized MgO in Al<sub>2</sub>O<sub>3</sub>-SiC composites were investigated. The overall changes in the density and mechanical properties of sintered samples (hardness, bending strength and toughness) were evaluated.

After mixing, drying and uniaxial compaction of the powders, they were first heat-treated at low temperature in an electric furnace to remove any residuals. They were then heat-treated at high temperature (1700 °C) inside a graphite furnace in argon atmosphere for sintering (at normal and high pressure). The content of MgO in the Al<sub>2</sub>O<sub>3</sub>-10 vol% SiC composite was 0, 500, 1000, and 1500 ppm.

The fracture toughness ( $K_{IC}$ ) of sintered composite with 10 vol% SiC (nano-sized) and different amounts of MgO was investigated by means of the Vickers indentation method. Microstructural analysis was performed using a scanning electron microscope.

The data showed that the mechanical properties were increased up to 1000 ppm MgO and then decreased above that. Microstructural observations revealed that in Al<sub>2</sub>O<sub>3</sub>-10 vol% SiC nanocomposites, nano-scale SiC particles were normally distributed all over the Al<sub>2</sub>O<sub>3</sub> matrix and inhibited the abnormal grain growth of Al<sub>2</sub>O<sub>3</sub>. In addition, transgranularly fractured alumina grains were observed on the fracture surface of the samples.

The results also showed that the fracture toughness of the composites with MgO was improved and better than that of Al<sub>2</sub>O<sub>3</sub>-10 vol% SiC samples.

*Keywords:* Nanocomposite, sintering, additive, mechanical properties, microstructure

### I. Introduction

Al<sub>2</sub>O<sub>3</sub> ceramics are widely used in many fields owing to their improved fracture strength, toughness, density and hardness<sup>1-2</sup>. There are several approaches to avoid abnormal growth of the alumina grains; one of them is through the addition of MgO<sup>3-5</sup>. A small amount of MgO can effectively inhibit the abnormal growth of the alumina grains. Another way is to add second-phase particles distributed throughout the samples<sup>6-7</sup>. Previous results have shown that making composites can improve the overall properties. For example, the addition of SiC nano-particles to an Al<sub>2</sub>O<sub>3</sub> matrix resulted in enhanced properties<sup>8-11</sup>. It has been observed that nano-sized SiC particles are effective in inhibiting the grain growth of alumina ceramics by pinning the grain boundaries and grain junctions after sintering at high temperature<sup>7-12</sup>. In alumina-silicon carbide nanocomposites, most of the researchers observed an intra/inter type of microstructure, in which most of the SiC particles, typically smaller than 0.2 μm, were predominantly dispersed within the matrix. Larger SiC particles are located in the grain boundaries and triple-point junctions. The results revealed that

the ultimate properties of a material depend on the microstructures developed during sintering. The sintering of undoped alumina to its theoretical density is very difficult. The major factors that hinder densification are abnormal grain growth and pore detachment from the grain boundaries during boundary migration. Applying small amounts of dopant, such as MgO could similarly inhibit the Al<sub>2</sub>O<sub>3</sub> grain growth. Residual stress is sometimes reported, which could be due to the thermal expansion between alumina and SiC particles, dislocations, sub-grain-boundary formation, and microcracking<sup>1-5</sup>. The important roles of MgO dopant in Al<sub>2</sub>O<sub>3</sub>-SiC nanocomposite seem to be:

- 1) Lowering the grain boundary mobility<sup>2</sup> and<sup>13-14</sup>,
- 2) Increasing the surface diffusivity along with higher pore mobility<sup>15-17</sup>,
- 3) Decreasing the grain boundary anisotropy<sup>18</sup>.

The objective of this work was to investigate the effects of adding a small amount of MgO (up to 1500 ppm) to alumina-based nanocomposites containing 10 vol% SiC particles.

\* Corresponding author: [nemati@sharif.edu](mailto:nemati@sharif.edu)

## II. Experimental

Very fine commercially available  $\gamma$ - $\text{Al}_2\text{O}_3$  (CR15, Baikowski Chemie, France), SiC powders (Bsc-21c, Performance Ceramics Company, Peninsula, OH, USA), and very high-purity magnesium oxide (>99.98 %) were used as the starting materials. The average particle sizes of  $\gamma$ - $\text{Al}_2\text{O}_3$  and  $\beta$ -SiC powders were 100 nm and 80 nm, respectively. The content of MgO particles in the  $\text{Al}_2\text{O}_3$ -10 vol% SiC was 0, 500, 1000, and 1500 ppm. After being ball milled, the samples were mixed in propanol for 3 h. They were then dried in an electric furnace to remove the propanol. The samples were sintered in a high-temperature graphite furnace in argon atmosphere at 1700 °C for 90 min. Finally, a few samples were hot-pressed in the range of 1500 to 1700 °C. The density of the samples was evaluated based on the Archimedes principle.

The sintered samples were then polished, using SiC papers and 1- $\mu\text{m}$  diamond paste. Vickers hardness measurement (Future tech FM-700) was performed on sintered and polished samples, with a load of 98 N for 30 s. For each load, at least five indentations were made, and the average indentation size and crack length parameters were measured. To reduce any possible effects of environmentally assisted cracking, the measurements were always made within 2 h of indentation. The hardness was calculated from the diagonal length of the impression, using Eq. (1):

$$H_V = (1.8544) (P/d^2) \quad (1)$$

where  $H_V$  = Vickers hardness,  $P$  = applied load (kg) and  $d$  = the diagonal length (mm) of nanocomposites based on Vickers indentation methods. Some indented samples were then polished, to identify the crack geometry as either median/radial or Palmqvist, and then  $K_{IC}$  was measured from the surface crack length, assuming that the crack geometry is the median/radial type. These are generally of the forms of Eqs. (2) and (3):

$$K_{IC} = \alpha (E/H)^n (P/c^{3/2}) \quad (2)$$

or

$$K_{IC} = \beta (P/c^{3/2}) \quad (3)$$

in which  $c$  is the measured as half of the total crack span around indentations made with a load  $P$ , in a material with Young's modulus  $E$  and hardness  $H$ , with varying pre-factors  $\alpha$  and  $\beta$  depending on the assumptions that have been made around the indentation stress field and  $n$  equal or close to 0.5. This method should be regarded with suspicion if the absolute value for the fracture toughness is derived. Even if the Vickers indentation method is used simply for comparative studies of materials, the possibility that the crack geometry could change from one material to another should be considered. In Eqs. (1) and (2) the cracks are generally assumed to be 'halfpenny', but this is not always or even often the case<sup>20</sup>. A further possibility is that the geometry of the crack may change more radically to the 'Palmqvist' type, typically found in tougher ceramics. Analysis of fracture toughness based on these results is discussed later.

After polishing and thermal etching of the samples sintered at 1450 °C for 1 h, microstructural analysis was performed with a scanning electron microscope.

The fracture surfaces of the sintered nanocomposites were used to calculate the average grain size of the samples, applying the linear intercept method (at least five lines per area). The average grain size,  $G$ , was then calculated using Eq. (4):

$$G = \frac{n}{M \cdot N \cdot L} \quad (4)$$

where  $n$  is a geometrically dependent proportionality constant (it was assumed that  $n=1.5$ ),  $L$  the total test line length,  $M$  is the magnification, and  $N$  is the total number of intercepts.

## III. Results and Discussion

Fig. 1 shows the relative density as a function of the MgO content in  $\text{Al}_2\text{O}_3$ -10 vol% SiC nanocomposite, sintered at 1700 °C for 1.5 h. The data indicated that the addition of 0–1000 ppm MgO could significantly increase the density of normally and hot-pressed sintered alumina-10 vol% silicon carbide nanocomposite. Further addition of MgO up to 1500 ppm did not improve the density. This finding was in accordance with the data reported by Wang *et al.*<sup>23</sup>.

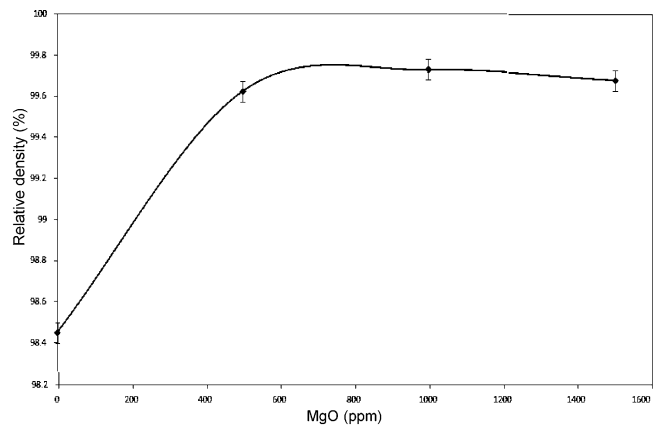
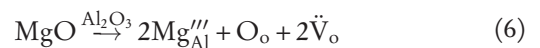


Fig. 1: Relative densities as a function of MgO content in  $\text{Al}_2\text{O}_3$ -10 vol% SiC nanocomposites sintered at 1700 °C for 90 min (at normal pressure).

It has been proposed that the role of MgO can be described as follows:

First, some part of MgO can diffuse inside the alumina particles, as the following reactions show (based on defect chemistry of MgO in alumina):



$\text{Mg}'_{\text{Al}}$  meaning that Mg cation is substituted to Al.

$\ddot{\text{V}}_o$  meaning the vacancy of oxygen.

$\text{Mg}_i$  meaning the Mg cation inter the interstitial sites.

$\text{O}_o$  meaning that oxygen goes to oxygen position.

$\text{Mg}'''_{\text{Al}}$  meaning the vacancy of Al.

Reaction (5) is likely to be the dominant reaction in the substitution. Accordingly, diffusion was enhanced and as a result of that, densification was improved.

Secondly, some parts of MgO are likely to modify the grain boundary of the system as well. For example, the undoped nanocomposite exhibits a relative density of 98.45,

compared to a relative density of 99.73 for the nanocomposite containing 1000 ppm MgO.

The theoretical density of alumina-10 vol% silicon carbide-magnesium oxide was calculated to be 3.91 g.cm<sup>-3</sup> based on the theoretical densities of  $\gamma$ -Al<sub>2</sub>O<sub>3</sub> (3.98 g.cm<sup>-3</sup>), silicon carbide and magnesium oxide (3.21 g.cm<sup>-3</sup>) and (2.8 g.cm<sup>-3</sup>), respectively. In the sample containing 1000 ppm and 1500 ppm MgO, the relative density was 99.62 and 99.68 %, respectively, which indicated either a constant or a small decrease in the density of the latter one.

It seems to us that the substitution of MgO in alumina is limited. The higher content of MgO is not the dominant mechanism for densification. It is likely that the extra MgO is located in the grain boundaries and acts as a grain growth inhibitor.

In order to study the effect of sintering pressure on relative density, an investigation was conducted between 10 and 30 MPa for 90 min on the hot-pressed samples at 1700 °C.

As shown in Fig. 2, in order to achieve densities of more than 99.6 %, a pressure of 30 MPa is required as well as a reduced grain size in the nanocomposite.

As seen in Fig. 3, the changes in the Vickers hardness (at 30 MPa) as a function of the MgO content were very similar to those of the relative density as function of the MgO content.

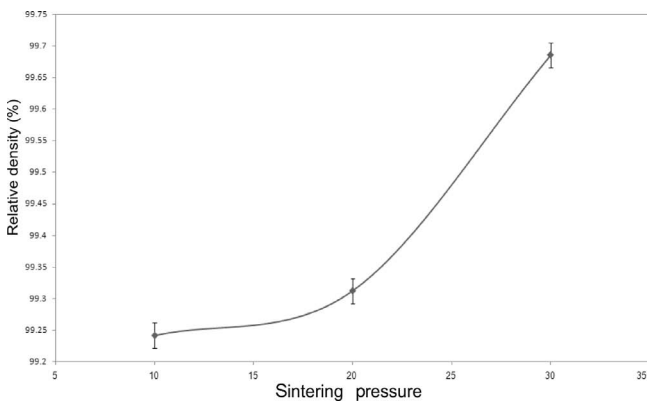


Fig. 2: Relative densities as a function of sintering pressure for nanocomposite containing 500 ppm MgO at 1700 °C sintered for 90 min.

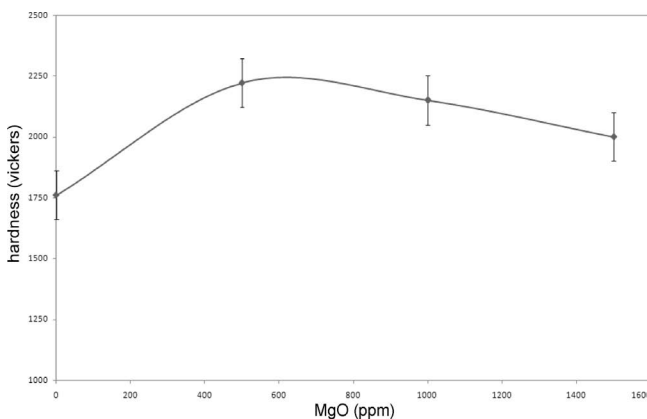


Fig. 3: Vickers hardness as a function of MgO content in Al<sub>2</sub>O<sub>3</sub>-10 vol% SiC nanocomposite sintered at 1700 °C for 90 min (at 30 MPa).

Vickers hardness increased with increasing MgO content up to 500 ppm, and then decreased with any further increase in the MgO content. In this case, the highest value for H<sub>V</sub> was obtained in the sample with 500 ppm MgO. The results indicated that for all doped samples, the H<sub>V</sub> values were higher than the undoped samples.

As it has already been proven, a denser ceramic nanocomposite exhibits a higher Vickers hardness than that of a porous one. It seems that an increase in the sintered density of nanocomposite with a small amount of MgO is the main reason and this is confirmed in Fig. 4. This figure shows the SEM micrographs of the fracture surfaces for the compositions containing 0, 500, 1000, and 1500 ppm MgO, respectively. Both the nano-sized SiC particles and MgO are expected to affect the sintering behavior of the alumina matrix. It sounds as if the former is effective in restricting the grain growth of alumina grains by pinning at the grain boundaries and grain junctions, as evidenced by the refinement in grain size observed in Al<sub>2</sub>O<sub>3</sub>-10 vol% SiC nanocomposites, in accordance with previous works 4,7. In the samples containing 1000 and 1500 ppm MgO, decreases in relative density and hardness as well as an increase in the grain size of the alumina particles were observed, as shown in Table 1. The average grain sizes of samples were calculated with the linear intercept method. As seen in Fig. 4 and Table 1, the Al<sub>2</sub>O<sub>3</sub> matrix grain size was decreased with the increase of the MgO content above 500 ppm.

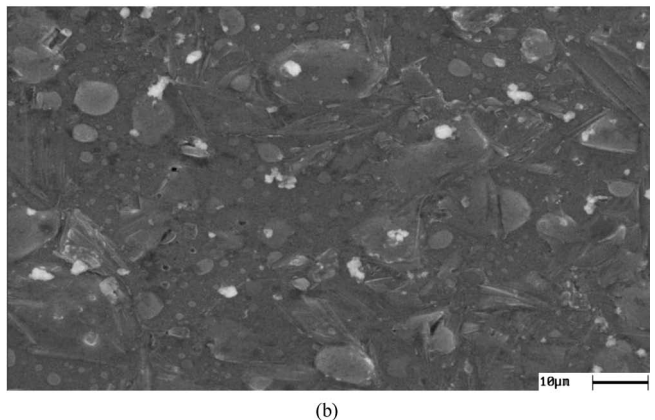
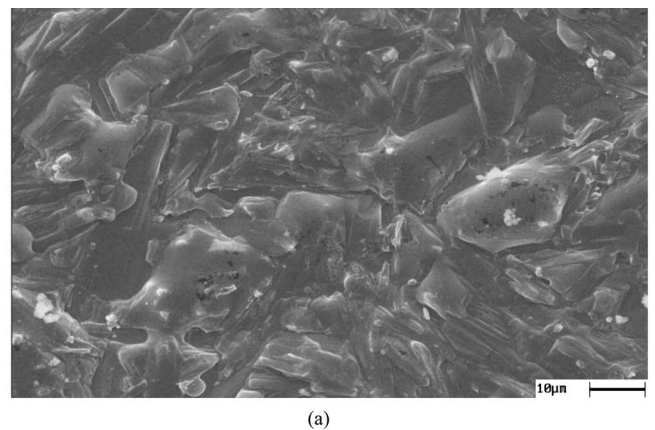
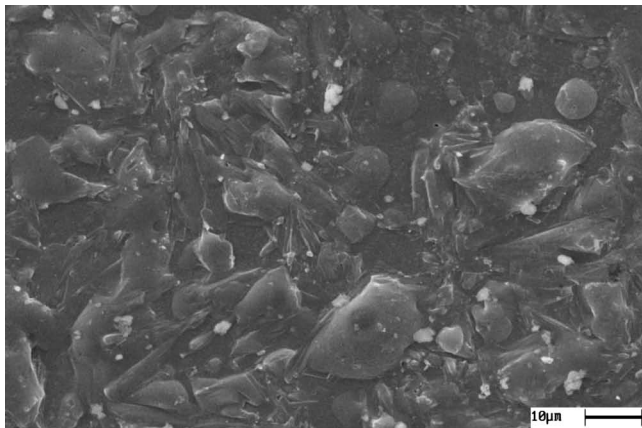
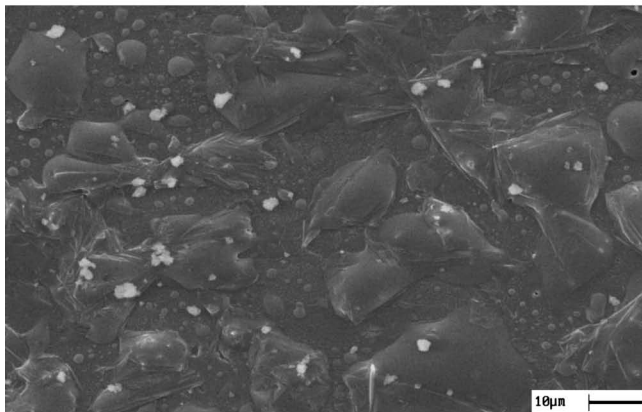


Fig. 4: SEM micrographs of the monolithic Al<sub>2</sub>O<sub>3</sub> and the composites (samples hot-pressed at 30 MPa): (a): without MgO, (b): with 500 ppm MgO.



(c)



(d)

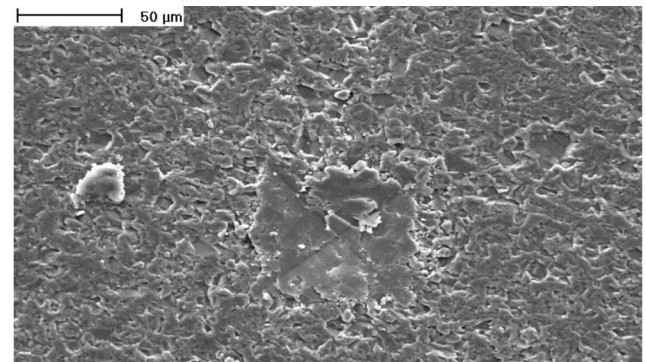
**Fig. 4:** SEM micrographs of the monolithic  $\text{Al}_2\text{O}_3$  and the composites (samples hot-pressed at 30 MPa): (c): with 1000 ppm MgO, and (d): with 1500 ppm MgO.

**Table 1:** The average grain size of samples calculated based on the linear intercept method (hot-pressed samples at 30 MPa)

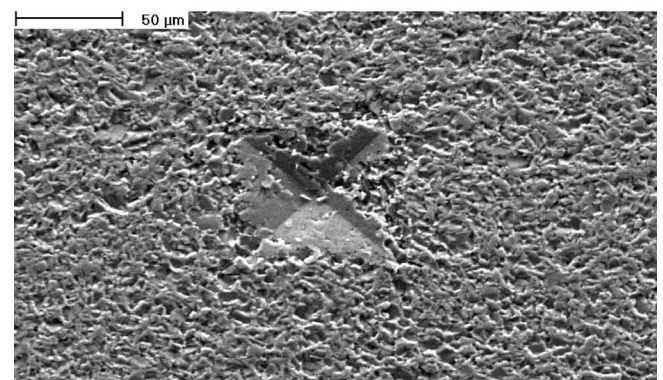
Sample	MgO wt%	Hot pressing temperature ( $^{\circ}\text{C}$ ) (at 30 MPa)	Time (min)	Average grain size of $\text{Al}_2\text{O}_3$ ( $\mu\text{m}$ )
A1	0	1700	90	$8.5 \pm 0.5$
A2	500	1700	90	$4.3 \pm 0.3$
A3	1000	1700	90	$4.7 \pm 0.3$
A4	1500	1700	90	$5 \pm 0.3$

Elemental distribution mapping indicated that nanoscale SiC particles were normally distributed throughout the  $\text{Al}_2\text{O}_3$  matrix (inside the  $\text{Al}_2\text{O}_3$  grains, on the boundaries as well as at the junctions of grains). These observations are in accordance with Niihara's classification. These observations indicated that most of the SiC particles, usually particles smaller than  $0.2 \mu\text{m}$ , were predominantly dispersed within the matrix grains. But, some larger SiC particles were dispersed at the grain boundaries and triple-point junctions<sup>1-2, 21-22</sup>. It is proposed that the most advantageous effect of SiC nanoparticles in an alumina matrix is their ability to refine the microstructure by restrict-

ing grain growth of the matrix alumina. The trace of the indenter on the surface and the crack type around the indentation are shown in Fig. 5.



(a)



(b)

**Fig. 5:** SEM images of indenter trace on the surface with the load of 98 N (samples sintered at normal pressure): (a) Alumina-10 vol% SiC, and (b) Alumina-10 vol% SiC-1000 ppm MgO.

Fig. 6 presents the hardness as a function of sintering pressure for nanocomposites containing 500 ppm MgO, sintered at  $1700^{\circ}\text{C}$  for 90 min. Considering the crack system to be in the forms of median/radial cracks types, the  $K_{\text{IC}}$  was calculated using Eqs. (1) and (2).

Calculation of Vickers indentation fracture toughness resulted in  $K_{\text{IC}}$  values of  $3-3.5 \text{ MPa}\cdot\text{m}^{1/2}$  for the alumina-10 vol% SiC and  $3.5-4.0 \text{ MPa}\cdot\text{m}^{1/2}$  for the samples containing MgO. These observations indicated that the  $K_{\text{IC}}$  of all studied materials was increased with crack length (i.e. higher loads); a behavior similar to that of materials with an 'R-curve' characteristic.

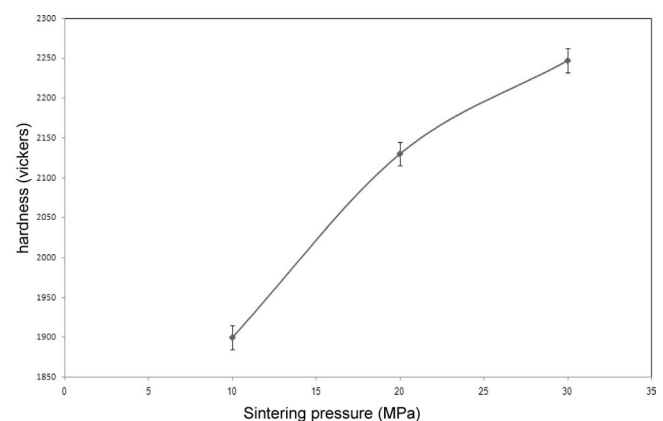


**Fig. 6 :** Hardness as a function of sintering pressure for nanocomposites containing 500 ppm MgO at  $1700^{\circ}\text{C}$  for 90 min.

Fig. 7 indicated that fracture toughness was improved with increasing sintering pressure from 10 to 30 MPa. Although those two mechanisms have been proposed for the effects of MgO in the system, the exact mechanism(s) behind the enhancement level of additives in composites still remain unclear. Other possible mechanisms of additive in such composites are:

- (1) A reduction in the number and size of processing-induced flaws; and
- (2) An improved response to grinding and polishing, resulting in a reduction in the number and size of polishing-induced flaws.

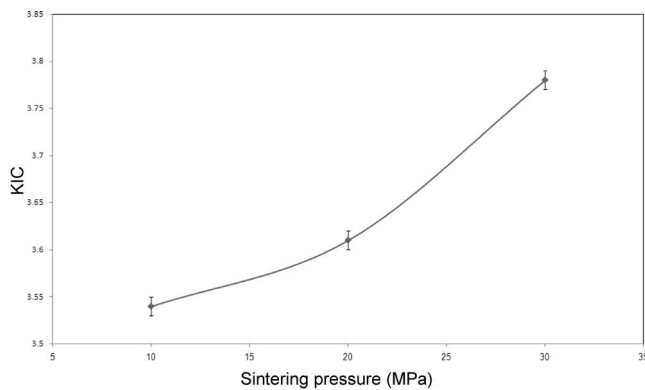


Fig. 7: K<sub>IC</sub> values as a function of sintering pressure for nanocomposite containing 1500 ppm MgO, sintered at 1700 °C for 90 min.

Fig. 8 shows that MgO addition has improved the toughness of the samples. As shown in Fig. 8, the toughness value of the samples containing 1500 ppm MgO was about 3.85 MPa.m<sup>1/2</sup> (at 30 MPa), which was more than that of the undoped nanocomposite (about 3.5 MPa.m<sup>1/2</sup>). As indicated in this figure, there is a significant change in the toughness values with the MgO content. However, the differences between the samples depend on using the appropriate equations and crack geometries. Given the uncertainties in the numerical pre-factors owing to the poorly defined indentation stress fields, the results from this type of test must thus be regarded with extreme caution.

As seen in Fig. 9, the observed fracture mode was mainly the transgranular fracture mode.

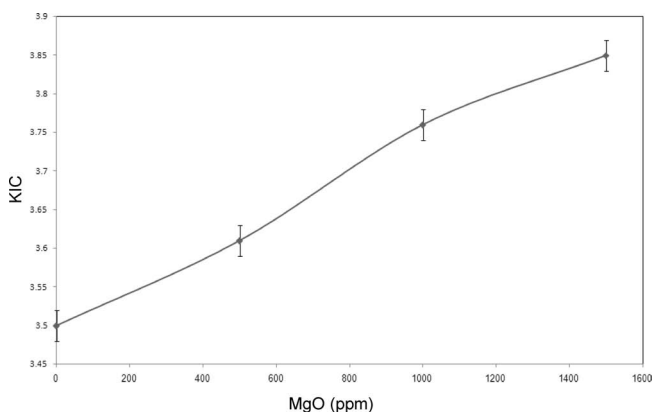


Fig. 8: K<sub>IC</sub> value as a function of MgO content in Al<sub>2</sub>O<sub>3</sub>-10 vol% SiC nanocomposites sintered at 1700 °C for 90 min (at 30 MPa).

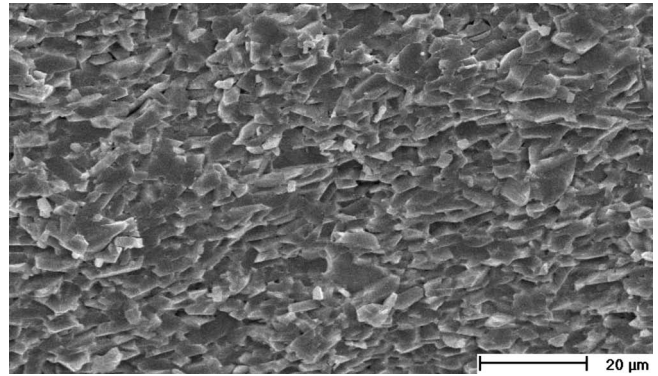


Fig. 9: Fracture surface of nanocomposite containing 1500 ppm MgO, sintered at 1700 °C for 90 min (at normal pressure).

#### IV. Conclusions

Alumina-10 vol% silicon carbide-magnesium oxide nanocomposites were prepared on the basis on an aqueous processing route.

A small addition of nano-sized MgO particles in ppm range to Al<sub>2</sub>O<sub>3</sub>-10 vol % SiC nanocomposite improves the bending strength, compared with that of Al<sub>2</sub>O<sub>3</sub>-10 vol% SiC with the same grain size.

The effects of such a small amount of MgO on the sintering and microstructural development of Al<sub>2</sub>O<sub>3</sub>-10 vol% SiC nanocomposite may be explained using the arguments which have been documented for the beneficial effects of a small amount of MgO in alumina ceramics.

Nanoscale SiC particles inhibited the grain growth of Al<sub>2</sub>O<sub>3</sub>, and decreased the size of the matrix grains.

The fracture mode of Al<sub>2</sub>O<sub>3</sub>-10 vol% SiC nanocomposites was observed to be mainly the transgranular fracture mode.

Mechanical properties (hardness and fracture toughness) were improved in comparison with undoped nanocomposites.

#### References

- 1 Niihara, K: New design concept of structural ceramics – ceramic nanocomposites, *J. Ceram. Soc. Jpn.*, **9**, 974, (1991).
- 2 Niihara, K., Nakahira, A., Sekino, T.: New nanocomposites structural ceramics, in: S. Komarneni, J.C. Parker, G.J. Thomas (Eds.), *Nanophase and Nanocomposite Materials*, Materials Research Society, Pittsburg, 405–412 (1993).
- 3 Zhao, J., Stearns, L.C., Harmer, M.P., Chan, H.M., Miller, G.A., Cook, R.F.: Mechanical behavior of alumina-silicon carbide nanocomposites, *J. Am. Ceram. Soc.*, **76**, [2], 503–510, (1993).
- 4 Stearns, L.C., Zhao, J., Harmer, M.P.: Processing and microstructure development in Al<sub>2</sub>O<sub>3</sub>-SiC nanocomposite, *J. Euro. Ceram. Soc.*, **10**, 473, (1992).
- 5 Bae, S.I., Baik, S.: Critical concentration of MgO for the prevention of abnormal grain growth in alumina, *J. Am. Ceram. Soc.*, **77**, [10], 2499–2504, (1994).
- 6 Lange, F.F., Hirlinger, M.M.: Hindrance of grain growth in Al<sub>2</sub>O<sub>3</sub> by ZrO<sub>2</sub> inclusions, *J. Am. Ceram. Soc.*, **67**, [30], (1984).
- 7 Sterns, L.C., Harmer, M.P.: Particle-inhibited grain growth in Al<sub>2</sub>O<sub>3</sub>-SiC: I, Experimental Results, II, Equilibrium and Kinetic Analyses, *J. Am. Ceram. Soc.*, **79**, [12], 3013–3028, (1996).

- 8 Zhao, J., Stearns, L.C., Harmer, M.P., Chan, H.M., Miller, G.A., Cook, R.F.: Mechanical behavior of alumina-sic nanocomposites, *J. Am. Ceram. Soc.*, **76**, [2], 503–510, (1993).
- 9 Chou, I.A., Chan, H.M., Harmer, M.P.: Machining induced surface residual stress behavior in  $\text{Al}_2\text{O}_3$ -SiC nanocomposites, *J. Am. Ceram. Soc.*, **79**, [9], 2403–2409, (1996).
- 10 Jang, B., Enoki, M., Kishi, T.: Control of microstructure of alumina ceramics by dispersion of nano SiC particulates, *J. Ceram. Soc. Jpn.*, **102** [9], 863–867, (1994).
- 11 Brook, R.J.: Fabrication principles for the production of ceramics with superior mechanical properties, *Proc. Br. Ceram. Soc.*, **32**, 74, (1982).
- 12 Wang, H.Z., Gao, L., Guo, J.K.: The effect of nanoscale SiC particles on the microstructure of  $\text{Al}_2\text{O}_3$  ceramics, *Ceram. Int.*, **26**, 391–396, (2000).
- 13 Bennison, S.J., Harmer, M.P.: Abnormal grain growth in sintering powder compacts, *J. Am. Ceram. Soc.*, **68**, (1985).
- 14 Burke, J.E., Lay, K.W., Procnazka, S.: The effect of MgO addition on mobility of grain boundaries and pores in aluminium oxide, *Mater. Sci. Res.*, **13**, 417, (1980).
- 15 Heuer, A.H.: Two kinds of roles of MgO in the densification and grain growth of alumina under various Atmospheres: sensitive and insensitive roles to the experimental procedures, *J. Am. Ceram. Soc.*, **62**, 317, (1979).
- 16 Roedel, J., Cilaeser, A.M.: Segregation of magnesium to the internal surface of residual pores in translucent polycrystalline alumina, *J. Am. Ceram. Soc.*, **73**, 3302, (1990).
- 17 Sung, C., Wei, G., Ostreicher, K.J., Rhodes, W.H.: Solubility of magnesia in polycrystalline alumina at high temperatures, *J. Am. Ceram. Soc.*, **75**, 1796, (1992).
- 18 Handwerker, C.A., Dynys, J.M., Cannon, R.M., Cable, R.L.: Pore drag and pore-boundary separation in alumina, *J. Am. Ceram. Soc.*, **73**, 1371, (1990).
- 19 Ponton, C.B., Rawling, R.D.: Vickers indentation fracture toughness Test: Part 1, *Mater. Sci. Tech.*, **5**, 865–872, (1989).
- 20 Cook, R.F., Pharr, G.M.: Direct observation and analysis of indentation cracking in glasses and ceramics, *J. Am. Ceram. Soc.*, **73**, [4], 787–817, (1990).
- 21 Sternitzke, M., Derby, B., Brook, R.J.: Alumina/Silicon carbide nanocomposites by hybrid polymer/powder processing microstructural and mechanical properties, *J. Am. Ceram. Soc.*, **81**, 41–48, (1998).
- 22 Levin, I., Kaplan, W.D., Brandon, D.G., Layyous, A.A.: Effect of SiC sub micrometer particle size and content on fracture toughness of alumina-siC nanocomposites, *J. Am. Ceram. Soc.*, **78**, 254–256, (1995).
- 23 Wang, J., Lim, S.Y., Ng, S.C., Chew, C.H., Gan, L.M.: Dramatic effect of small amount of MgO addition on the sintering of  $\text{Al}_2\text{O}_3$ -5 vol% SiC nanocomposites, *Mater. Lett.*, **33**, 273–277, (1998).